Eur Biophys J (1995) 24: 99–106

European Biophysics Journal

Electrical impedance analysis in plant tissues: on the biological meaning of Cole-Cole α in Scots pine needles

M. I. N. Zhang[1,*], T. Repo[2], J. H. M. Willison[1], S. Sutinen[3]

[1] Department of Biology, Dalhousie University, Halifax, N.S. Canada B3H 4J1
[2] Faculty of Forestry, University of Joensuu, P.O. Box 111, FIN-80101 Joensuu, Finland
[3] The Finnish Forest Research Institute, Suonenjoki Research Station, FIN-77600 Suonenjoki, Finland

Received: 23 August 1994 / Accepted in revised form: 20 July 1995

Abstract. Electrical impedance spectra (80 Hz–1 MHz) in Scots pine needles were found to be characterized by spectrum skewness in the Cole-Cole plot. These spectra were subjected to analysis with two distributed models: (i) the Cole-Cole function and (ii) an equivalent circuit which takes account of the presence of air spaces within the needles (Model-A). In analysis with untreated needles (without artificial infiltration with water), Model-A fitted better than the Cole-Cole function to the experimental data. After infiltration of water into the needles, the extent of spectrum skewness was substantially decreased compared with the pre-infiltration condition and the Cole-Cole function fitted better than Model-A to the measured impedance data. The Cole-Cole α decreased from 0.47 in non-infiltrated needles to 0.42 in the infiltrated needles. The exceptionally large value of α in non-infiltrated needles can be explained by the presence of air spaces, which produce transmission line properties in the mesophyll. In support of the validity of Model-A, this new model provided specific membrane resistances of $1190 \pm 83\ \Omega\,cm^2$ in cold hardened and non-hardened needles respectively. These specific membrane resistance are comparable with previous reports of membrane resistances in other biological systems. It is concluded that in this exceptionally spongy tissue, Cole-Cole α is likely to be due to the effects of the transmission line properties of cells which are surrounded by air spaces and only thin cell walls outside the insulating cell membranes.

Key words: *Pinus sylvestris L.* (Scots pine) – Electrical impedance – Membrane capacitance – Transmission line – Cole-Cole α – Air space

* *Present address:* Department of Integrative Biology, University of Texas, Houston Medical School, 6431 Fannin, Houston, TX 77030, USA

Correspondence to: T. Repo (Tel.: +358 73 151 4093, Fax: +358 73 151 4444, e-mail: vtrepo@METSA1.joensuu.fi)

1. Introduction

Information of fundamental value in the physiology of organisms can be obtained by measuring the impedance spectra of tissues and organs (reviewed by Cole 1968; Ackmann and Seitz 1984). In simple tissues such as potato tuber tissue, the application of lumped electrical models (e.g. Hayden et al. 1969; Zhang and Willison 1991, 1993) has provided useful physiological information. In more complicated tissues such as woody stems, the tissue is better modelled by the impedance level Cole-Cole function (see Repo and Zhang 1993) as described in Eq. (1) (in materials science, it is usually called ZC or ZARC response function, see Macdonald 1987, pp. 16–20).

$$Z_c = R_\infty + \frac{R_o - R_\infty}{1 + (j\omega\tau_c)^{(1-\alpha)}} \quad (1)$$

Generally, the Cole-Cole function provides a good fit to a wide range of biological tissues (see Cole 1932, 1933, 1941) and it has thus been used frequently in characterizing the impedance of biological tissues (e.g. Schanne and P.-Ceretti 1978; Greenham et al. 1980, 1982; Ackmann and Seitz 1984; Mørkrid and Qiao 1988; Thomas et al. 1992; Repo and Zhang 1993). In this relationship, R_∞ is the tissue resistance at extremely high frequency, R_o is the impedance measured at extremely low frequency and corresponds to extracellular resistance, τ_c is a generalized time constant, and α is a factor within the range of 0–1 which describes the time constant distribution in the system.

Among the 4 parameters in Eq. (1), α is the least understood (Cole 1968; see Ackmann and Seitz 1984; Foster and Schwan 1989). Classically, α has been associated with an impedance phase angle $[(1-\alpha)\ \pi/2]$ which appears in the Cole-Cole plot and is due to cellular membranes (see Cole 1932, 1933, 1941, 1968). Although several decades have passed since Cole's work, the α in the Cole-Cole function (Cole-Cole α) is still not completely understood.

If each cell is represented by a single time constant circuit, a tissue with normally distributed cell sizes should be represented by a circuit with normally distributed time

constants in series. In a simulation at admittance level (at which α is the same as that at the impedance level), the admittance loci of a normally distributed time constant circuit was not an arc but almost a full semicircle (see Kanai et al. 1987), i.e. the α is quite close to 0. As α is usually found to be far larger than 0 in real measurements, this suggests that cell size distribution had little effect on α. At dielectric level, it has been speculated that α may relate to cell size distribution, the influence of cell organelles, cell packing, cell shapes and the influence of intercellular junctions (see Foster and Schwan 1989). In simulation (Foster and Schwan 1989, pp. 77–82), the Cole-Cole function requires almost a log-normal distribution of time constants in order to produce observed values of α. In biological systems, one does not expect cell sizes to vary by 100 to 1000 times within one tissue. At the dielectric level in yeast cell suspension cultures, Markx and co-workers (1991) found that real cell size distribution did not account for measured α. For these reasons it seems that cell size distribution is not likely to be a major factor in determining Cole-Cole α, and other causes must be sought for understanding its biological meaning.

In biological tissues, α is usually in the range of 0–0.4. This range of α corresponds to a membrane phase angle of 90° to 55° (for a list of membrane phase angles in tissues, see Cole 1933, p. 113; for a list of membrane phase angles in single cells, see Cole 1941). In our recent experiments with Scots pine needles (see Repo et al. 1994), α was found to be 0.47, which is exceptionally large. For theoretical reasons, we considered that this high value may be connected with the large amount of air space within pine needles. In the following, based on both experiments and theory, we explore the relationship between pine needle air spaces and the skewness in the measured spectrum which gives rise to the exceptionally large α. It is argued that this special case illuminates the general meaning of Cole-Cole α.

2. Theory

It was shown previously that there is a great difference in the ratio of extracellular to intracellular resistance (r_e/r_i or R_e/R_i) between the stems and the needles in Scots pine seedlings (Repo et al. 1994). In stems, the ratio averages 6.9 (7.3 and 6.4 for non-hardy and hardy tissues, respectively), whereas in needles this ratio averages 26.0 (15.5 and 36.5 for non-hardy and hardy tissues, respectively). We hypothesize that the large difference in R_e/R_i is due to the presence of extensive air space in the needles.

The proportion of the air spaces to mesophyll tissue in Scots pine needles is approximately 25% (volume/volume) (Soikkeli 1981) (see Fig. 1). By infiltrating the needles with water, we found that fresh weight increased by 15.5%, indicating that air space occupies a minimum of 15.5% (volume/volume). The difference between these two estimates is probably due to incomplete infiltration with water. By contrast, the woody stems have virtually no air space.

The path of a hypothetical electrical current in a spongy mesophyll system is described in Fig. 2. Where there are

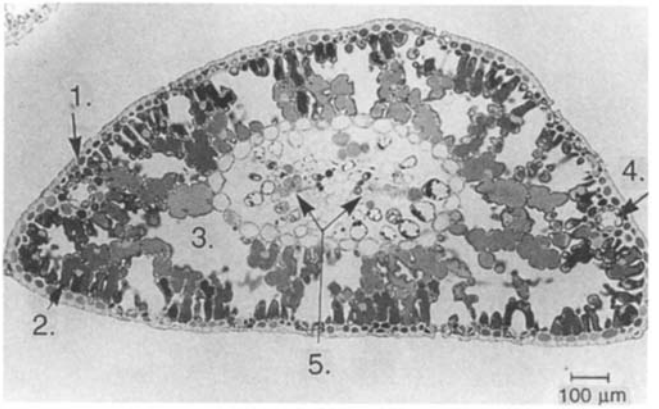

Fig. 1. Light micrograph of a Scots pine needle showing the epidermis (1), mesophyll tissue (2) with intercellular spaces (3), resin duct (4), and the conducting tissue with vascular bundles (5). ×78

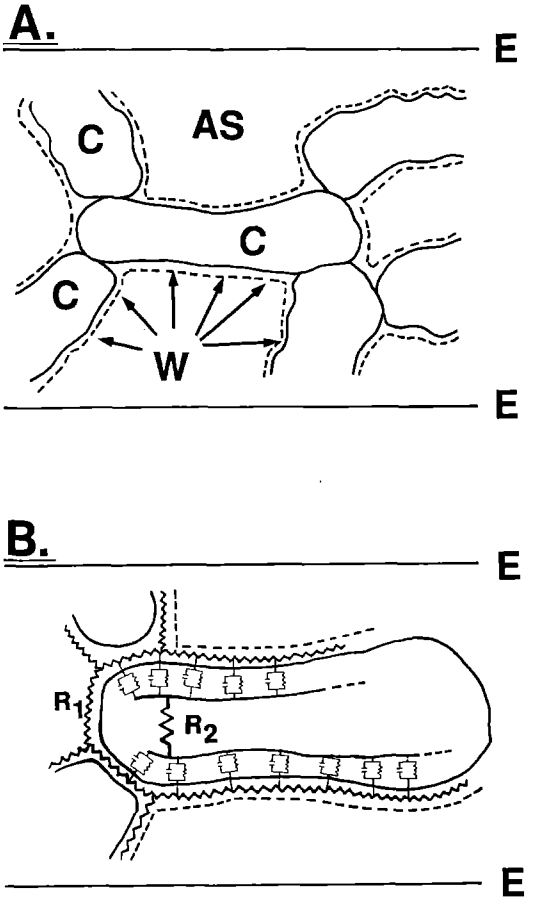

Fig. 2. **A** Mesophyll cells in Scots pine needles. AS – air space; *C* – cell; W – wet cell wall on the surface of mesophyll cell (arrow heads); E – electrode. **B** A mesophyll cell and its equivalent circuit. Extracellular resistance (R_1), intracellular resistance (R_2) and transmission line property of the system are indicated. E – electrode

a lot of air spaces, many mesophyll cells are partially surrounded by a layer of thin wet cell walls (Fig. 2 A). Because the amount of cell wall space available for current flow is small adjacent to the air spaces, the extracellular resistance will be higher than usual and most of the current in this part of the circuit can be expected to pass across

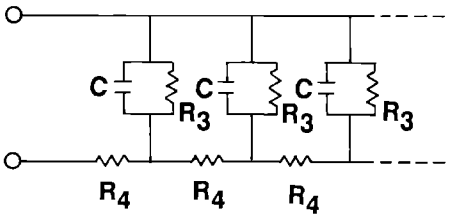

Fig. 3. An infinitely long transmission line representing plasma membrane property. C – specific membrane capacitance; R_3 – specific membrane resistance; R_4 – lateral resistance of water film in a unit area of cell surface

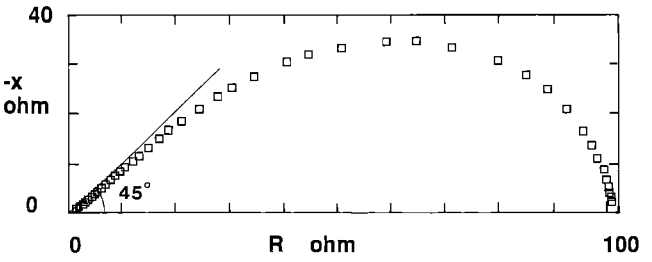

Fig. 5. A Cole-Cole plot of (3) with $A_o = 50$ and $\tau_m = 1$ millisecond. The frequency range is from 10 Hz to 800 kHz (from right to left, anti-clockwise). The characteristic frequency (f_c') is 276 Hz. R and –X are real and imaginary levels respectively. At the highest frequencies, the spectrum forms a 45 degree angle in relation to R axis

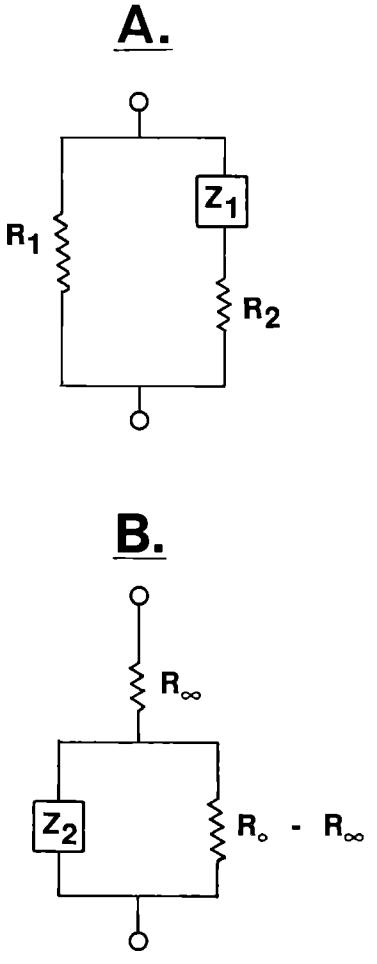

Fig. 4. A An equivalent circuit for a single mesophyll cell or piece of mesophyll tissue. R_1 – Extracellular resistance; R_2 – intracellular resistance, and Z_1 – membrane with transmission line property. **B** A transformed circuit from that in Fig. 4 A (see Appendix 3), which illustrates R_o and R_∞ in (5 b)

the cell membrane through a distributed circuit (see Fig. 2 B; and for detail, see Fig. 3).

In mesophyll cells, the vacuole is an important organelle which occupies most of the space within a cell (Fig. 1). In an ideal electrical model, the properties of the vacuole (tonoplast capacitance and vacuole interior resistance) should be included. In the model used here, for simplicity, the cell is treated as having one intracellular resistance (R_2) (Fig. 2 B). For present purposes, this simplified version of the modelling has the advantage of being directly comparable with the commonly used Cole-Cole function. In future, it may be possible to expand the model to include more details.

That part of a mesophyll cell which is surrounded by air space can be represented by a distributed circuit model which approximates an infinitely-long transmission line (Fig. 3). In this model (Fig. 3), the R_3 is specific membrane resistance ($\Omega\,\mathrm{cm}^2$), C is specific membrane capacitance ($\mathrm{F/cm}^2$), and R_4 is lateral resistance along a 1 cm^2 membrane surface area (ohm). The extracellular resistance (R_1) is a function of the wet layer associated with the cell walls surrounding the cells. Where there is a sufficiently thick wet layer, the extracellular resistance is low and the electrical current remains within this extracellular space. If the cell wall and its associated water forms a sufficiently thin layer over the cell surface, as when cells are surrounded by air spaces, the dominant factor affecting current flow is the leakiness of the cell membrane and the current is distributed across the cell membrane (Fig. 3). Under these circumstances, the extracellular resistance is described by R_4 (Fig. 3) and the membrane behaves like a transmission line.

Following a procedure described by Raistrick (1987, pp. 81–82), the impedance of the transmission line (Fig. 3) can be expressed as:

$$Z_t = \left(\frac{R_4 R_3}{1 + j\omega C R_3} \right)^{0.5} \tag{2a}$$

or

$$Z_t = \frac{A_0}{(1 + j\omega\tau_m)^{0.5}} \tag{2b}$$

in which $A_0 = (R_4 R_3)^{0.5}$ and $\tau_m = R_3 C$ (membrane time constant). For the derivation of Eq. (2 a), see Appendix 1.

Z_1 in Fig. 4 A is equal to two Z_t's in series (see Fig. 2 B) and therefore the impedance of an individual mesophyll cell is

$$Z_1 = \frac{2A_0}{(1 + j\omega\tau_m)^{0.5}} \tag{3}$$

Figure 5 illustrates the behavior of (3) as frequency varies. Within the commonly used frequency range, a skewed spectrum is produced. If the skewed spectrum is approximated by a semicircle as generated by (1), the center of the Cole-Cole plot will be depressed below the real axis. At extremely low frequency, Eq. (3) produces a maximum resistance of $2A_o$ and zero reactance. At extremely high frequency, Eq. (3) provides resistance and reactance val-

ues of zero. When $\omega\tau = 3^{0.5}$ the reactance attains its maximum value of $A_o/2^{0.5}$, and the resistance is $A_o\,(3/2)^{0.5}$. If we define the characteristic frequency (f_c') as the frequency at which maximal reactance is reached, as is conventional when using the Cole-Cole function (Eq. (1)), then $f_c' = 3^{0.5}\,(2\Pi\tau_m)^{-1}$ (see Appendix 2). As $\omega\tau_m$ becomes progressively larger than 1 with increasing frequency, Eq. (3) will approach a constant phase element (CPE) with a 45 degree phase angle (see the left half of spectrum in Fig. 5). With the Z_1 component in the circuit in Fig. 4 A, the total circuit represents a cell. In a tissue with m cell layers along the direction of the electrical field and n cells within each cell layer, the Z_1 component in the circuit in Fig. 4 A will be

$$Z_1 = \frac{(m/n)\,2A_0}{(1 + j\,\omega\,\tau_m)^{0.5}} \tag{4}$$

and this represents the whole tissue.

The circuit in Fig. 4 A is equivalent to a mesophyll cell or cells in a pine needle. It can be conveniently replaced by the circuit in Fig. 4 B for impedance analysis by complex non-linear least squares (CNLS) curve-fitting. The advantage of using the circuit in Fig. 4 B is that R_o and R_∞ [see Eq. (5 b) below] can be graphically displayed in the complex impedance locus, whereas the components of the circuit in Fig. 4 A are better revealed by plotting at the admittance level. The two circuits in Fig. 4 A and 4 B are interconvertible and both circuits can have exactly the same impedance response at all frequencies (see Cole 1928, p. 34; Macdonald 1987, p. 11, Appendix 3).

The total impedance of the circuit in Fig. 4 B is

$$Z = R_\infty + \frac{R_o - R_\infty}{1 + \dfrac{R_o - R_\infty}{2A_o'\,(m/n)}\,(1 + j\,\omega\,\tau_m)^{0.5}} \tag{5a}$$

in which $A_o' = A_o/(1 + R_2/R_1)^2$ (see Appendix 3 for detail), or

$$Z = R_\infty + \frac{R_o - R_\infty}{1 + \beta\,(1 + j\,\omega\,\tau_m)^{0.5}} \tag{5b}$$

in which

$$\beta = \frac{R_o - R_\infty}{2A_o'\,(m/n)}.$$

In the following, let us call (5 b) Model-A[1] (in which A stands for air space).

3. Experiments

Impedance spectral measurements (80 Hz–1 MHz) were made in 15 mm long sections (taken from the middle) of 15 previous-year needles of Scots pine (*Pinus sylvestris* (L.)) taken randomly in their frost hardy stage (March 1994 in Finland), both before and after infiltration with water (for measurement method, see Repo 1994). By using Ag/AgCl electrodes (WPI Ltd., RC 1) which were set in contact with a conductive paste to form a salt bridge between electrode and sample, and by the short-circuit correction operation of the LCR measurement instrument (HP4284A), electrode/tissue interface polarization is kept to a minimum (see Repo 1994 for detail). The spectra thus measured were analyzed with both the Cole-Cole function and Model-A by a BIA program (Bio-Impedance Analysis v. 3.0, written in Microsoft Visual Basic). In addition, impedance spectra of 16 current-year needles of Scots pine taken randomly at two cold hardening stages (August 1992 and October 1992) (for detail, see Repo et al. 1994) were analyzed.

The relative goodness of fit of the two models (Cole-Cole and Model-A) was tested using root mean squared differences (RMSD) between best-fit model data and measured data. As both models contain 4 free parameters, the general fit can be revealed by direct comparison of RMSDs. In addition, since the curve-fitting program displays in dynamic graphics the best-fit curve together with experimental data an absolute best-fit is guaranteed.

The Cole-Cole function fits reasonably well in a typical impedance spectrum of non-infiltrated needles (Fig. 6 A). However, a much better fit is obtained by Model-A whose prediction almost completely overlaps with the experimental data (Fig. 6 B). The best fit of Model-A in Scots pine needles without infiltration with water produced smaller RMSD than the Cole-Cole function in 44 of a total of 47 cases (both non-hardened and hardened samples). In a typical fit, the relative error (stan-

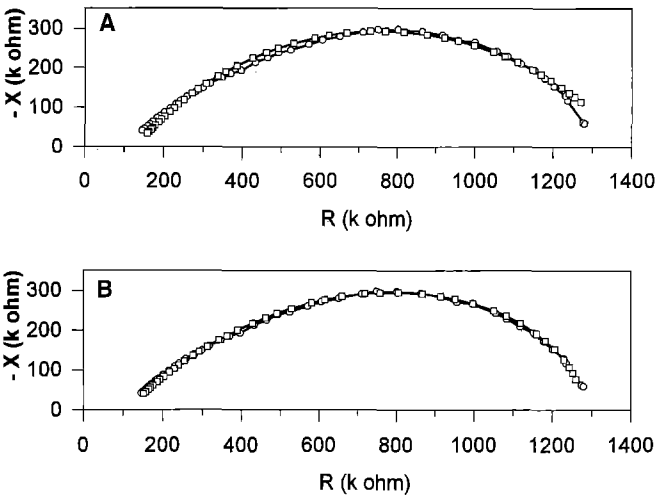

Fig. 6. Cole-Cole plot of a typical impedance spectrum of a non-hardy Scots pine needle and the best fit by the Cole-Cole function **A** and the Model-A **B**. R and X are real and imaginary parts of impedance respectively. The best fit Cole-Cole function parameters (±SE) are: $R_\infty = 129$ (±6.5) kΩ, $R_o = 1385$ (±15) kΩ, $\tau = 60.1$ (±2.6) μs, $\alpha = 0.44$ (±0.01) (RMDS = 20251). The best fit Model-A parameters are: $R_\infty = 109$ (±3.1) kΩ, $R_o = 1605$ (±18) kΩ, $\tau_m = 1.28$ (±0.12) ms, $\beta = 0.28$ (±0.02) (RMSD = 10462). The empty circles are experimental data, and the empty squares are best-fit

[1] The R_∞ in Model-A has the same meaning as in the Cole-Cole function, i.e. resistance at extremely high frequency. However, unlike in the Cole-Cole function, due to the transmission line property of Z_2, the resistance of Model-A at extremely low frequency is equal to $(R_o + \beta R_\infty)/(1+\beta)$. Nevertheless, we kept R_o for a structural similarity to the Cole-Cole function.

Table 1. Cole-Cole α and the other parameters in the Cole-Cole function in Scots pine needles before and after water infiltration ($n=15$)

Treatment	R_∞ (kΩ)	R_o (kΩ)	τ_c (μs)	1-α
Non-infiltrated	222 ± 7	1920 ± 60	25.9 ± 0.4	0.533 ± 0.002
Infiltrated	121 ± 4	1230 ± 40	17.9 ± 0.3	0.583 ± 0.003
Significance	***	***	***	***

*** Indicates significant difference at $P<0.001$ between non-infiltrated and infiltrated

Table 2. Model-A parameters in Scots pine needles both with and without water infiltration ($n=15$)

Treatment	R_∞ (kΩ)	R_o (kΩ)	β	τ_m (ms)
Non-infiltrated	200 ± 7	2040 ± 60	0.136 ± 0.005	1.73 ± 0.12
Infiltrated	78 ± 3	1380 ± 40	0.186 ± 0.007	0.75 ± 0.04
Significance	***	***	***	***

*** Indicates significant difference at $P<0.001$ between non-infiltrated and infiltrated

Table 3. Best-fit parameter values of Model-A in Scots pine needles at non-hardy and hardy stages ($n=16$) (see Repo et al. 1994)

Treatment	R_∞ (kΩ)	R_o (kΩ)	β	τ_m (ms)
Non-hardy	95 ± 3	1550 ± 80	0.33 ± 0.03	1.3 ± 0.2
Hardy	113 ± 7	1980 ± 120	0.223 ± 0.011	1.19 ± 0.08
Significance	*	*	**	NS

NS–not significant
* – Significant at $p<0.05$
** –Significant at $p<0.01$

dard error/parameter value) of R_∞ decreased from 6.5% in the Cole-Cole model to 3.1% in the Model-A (see legend of Fig. 6). The relative error for R_o did not change significantly between the two models. τ_c and α in Cole-Cole model have different meanings than τ_m and β in Model-A, and therefore comparison of these parameters between models will not be meaningful. By contrast to the non-infiltrated needles, the Cole-Cole function produced smaller RMSDs than the Model-A after infiltration with water (total of 15 cases).

The analysis of previous-year Scots pine needles showed that all parameters in the Cole-Cole function changed significantly relative to controls following infiltration with water (Table 1). The parameters R_∞, R_o and τ_c decreased, but (1-α) increased. When the same data were analyzed by using Model-A, similar relative trends were found in R_∞ and R_o, the parameter β increased, and τ_m decreased (Table 2). During hardening, both of the resistances in Model-A increased but β decreased. The time constant τ_m was unchanged (Table 3).

4. Discussion

In impedance analysis of non-biological materials, an empirical function by Havriliak-Negami (HN) in the form of

$$Z_{HN}(\omega)=\frac{R_{HN}}{\{1+(j\omega\tau)^{1-\alpha}\}^{1-\beta}} \quad (6)$$

is often used for describing a skewed spectrum (see Havriliak and Negami 1966; Macdonald 1991; Repo et al. 1994). The HN function reduces to the Davidson-Cole function when $\alpha=0$ (Davidson and Cole 1951) and to the Cole-Cole function when $\beta=0$. These functions have similarities in appearance to the proposed Model-A. However, the selection of a good model should not be based only on its good curve-fit to experimental data, but more importantly on how to interpret each function parameter in biological terms. In the case of the HN function, the Davidson-Cole function or the Cole-Cole function, which are all empirical, it is difficult to interpret all their parameters in biological terms. By contrast, the Model-A describes a basic process – the distributed current flow along the mesophyll cell surface, and it helps us to understand the meaning of Cole-Cole α.

In this study, Model-A generally provided a better fit than the Cole-Cole function to the experimental data in the Scots pine needles that were not infiltrated with water (Fig. 6). The advantage of Model-A is not only its improved fit to experimental data compared with the widely used Cole-Cole function but, more importantly, its better defined set of model parameters. A benefit of this better definition is that membrane resistance can be calculated. If we assume a specific membrane capacitance of 1 $\mu F/cm^2$, we get estimates for membrane resistance ($R_3=\tau_m/C$) of hardy and non-hardy needles of 1190±83 $\Omega\,cm^2$ and 1323± 213 $\Omega\,cm^2$ respectively. We can have confidence in the method of obtaining these values because they are in the range around 1000 Ω generally found in many biological membranes (see Cole 1968, p. 103).

Further support for the validity of model-A comes from the experimental results. By infiltrating the needles with water, the "thin-wet-cell-wall" condition used in the Theory was removed. In support of the Theory, water infiltration altered the tissue property in such a way that the fit of Model-A was worse than the fit of the Cole-Cole function.

A major difference between Model-A and the Cole-Cole function is that α in the Cole-Cole function is not present in Model-A. Its loss is compensated for by the constant power factor, 0.5. A new variable, β, appears in Model-A. It controls both the skewness of the spectrum and the depression of the locus centre. Generally, a smaller β is associated with a more symmetric arc and a more depressed locus centre (larger α). When the spectra in Fig. 7 are curve-fit with the Cole-Cole equation, the α values are 0.464, 0.430, and 0.385 for β values of 0.1, 0.3 and 1.0, respectively. With large membrane phase angles at large β values, the spectrum is more asymmetric (Fig. 7C). Theoretically, when β approaches 1, at high frequencies ($\omega\tau>>1$), Model-A approaches the Cole-Cole function with an α close to 0.5. In the current experiments, β (0.14 to 0.33) was found to be much smaller than 1. It is there-

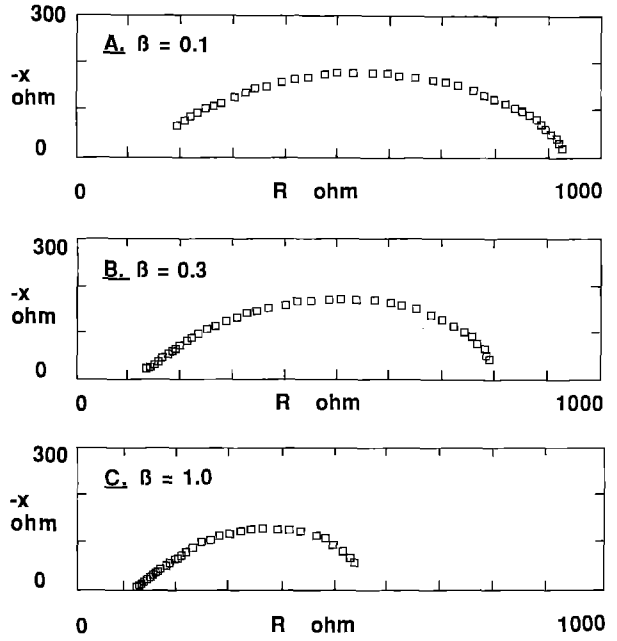

Fig. 7 A–C. A plot of Model-A (5 b) with $R_\infty = 100\ \Omega$, $R_o = 1000\ \Omega$ and $\tau_m = 1$ ms. β-values: 0.1 **A**, 0.3 **B** and 1.0 **C**. Frequency range: 100 Hz – 800 kHz (from right to left, anti-clockwise). When these spectra were analyzed with the Cole-Cole equation, the α values were 0.464, 0.430, and 0.385 for β values of 0.1, 0.3 and 1.0, respectively

fore clear that Model-A behaves quite differently in relation to frequency than does the Cole-Cole function.

The mesophyll cells within a needle are heterogeneously arranged (Fig. 1). It would be impossible to produce an electrical model which includes all the cell and tissue details. We can only expect to take account of the dominant tissue features. Since Model-A provided a reasonably good fit to the experimental data, the assumptions about AC current flow in the tissue and at the membrane level presented in the Theory section is supported and the model appears suitable for use in impedance analysis.

In an experimental system where errors are permitted, it can be difficult to distinguish the response differences between the Cole-Cole function and Model-A without knowing about the electrophysiological process involved. Even when a spectrum is actually determined by Model-A, the spectrum can nevertheless be fitted fairly well by the Cole-Cole function. Nevertheless, it has been possible to demonstrate that in this special case of Scots pine needles described here, Model-A is a better model than the Cole-Cole function for describing non-infiltrated needles, and the Cole-Cole function is a better model for infiltrated needles.

The analysis described in this study suggests that in many previous cases where tissues were modelled reasonably well by the Cole-Cole function, there may be an improved fit with alternative models, such as Model-A, which considers electrophysiological processes in more detail. In the present analysis, the exceptionally large Cole-Cole α is likely to be associated with the transmission line properties of some suspended mesophyll cells. While the analysis in the Scots pine needles is a special case in terms of tissue structure, it draws attention to the possibility of understanding the meaning of the Cole-Cole α in a general sense. Since many tissues do not have air spaces, the question remains unanswered as to why so many tissues have a membrane phase angle smaller than 90°. Perhaps tissues display some level of transmission line property even in the absence of air spaces. Alternatively, a complex of variables may contribute to α, of which the transmission line factor is dominant where air spaces are extensive.

Acknowledgements. The authors thank Dr. J. R. Macdonald in the Dept. of Physics and Astronomy, University of North Carolina, for comments on the analysis part. This study was founded by the Natural Sciences and Engineering Research Council (NSERC) of Canada to Dr. J. H. M. Willison and by the Academy of Finland to Dr. T. Repo.

List of symbols

Symbol	Unit	Meaning
$Z = Z' + jZ''$	Ω	impedance
Z'	Ω	resistance
Z''	Ω	reactance
j		complex number operator, $(-1)^{0.5}$
f	Hz	alternating current frequency
$\omega = 2\pi f$	rad/s	angular frequency
τ	s	time constant
Z_c	Ω	impedance in the Cole-Cole function
R_o	Ω	Z' measured at extremely low frequency in the Cole-Cole function
R_∞	Ω	Z' measured at extremely high frequency in the Cole-Cole function
τ_c	s	time constant in the Cole-cole function
$f_c = (2\pi\tau_c)^{-1}$	Hz	characteristic frequency at which $-Z''$ is maximum in Cole-Cole function time constant distribution factor in Cole-Cole function
$\pi(1-\alpha)/2$	rad	membrane phase angle in the Cole-Cole function
Z_t	Ω	transmission line property of membrane in Scots pine needle
R_1	Ω	extracellular resistance
R_2	Ω	intracellular resistance
R_3	$\Omega\,\mathrm{cm}^2$	specific membrane resistance
R_4	Ω	lateral resistance of water film around mesophyll cell surface
C	$\mu\mathrm{F/cm}^2$	specific membrane capacitance
$\tau_m = CR_3$	s	membrane time constant in Model-A
$f_c' = 3^{0.5}(2\pi\tau_m)^{-1}$	Hz	characteristic frequency for Z_t
β		a factor in Model-A controlling spectrum skewness and impedance locus center depression

References

Ackmann JJ, Seitz MA (1984) Methods of complex impedance measurement in biological tissue. CRC Crit Rev Biomed Eng 11:281–311

Cole KS (1928) Electric impedance of suspensions of spheres. J Gen Physiol 12:29–36

Cole KS (1932) Electric phase angle of cell membranes. J Gen Physiol 15:641–649

Cole KS (1933) Electric conductance of biological systems. Cold Spring Harbor Symp Quant Biol 1:107–116

Cole KS (1941) Impedance of single cells. Tabulae Biol 19 (Cellula, Pt. 2):24–27
Cole KS (1968) Membranes, Ions and Impulses, University of California Press, Berkeley and Los Angeles
Davidson DW, Cole RH (1951) Dielectric relaxation in glycerine. J Chem Phys 18:1417
Foster KR, Schwan HP (1989) Dielectric properties of tissues and biological materials: a critical review. CRC Crit Rev Biomed Eng 17:25–104
Greenham CG, Groves RH, Muller WJ (1980) Variation between populations of one form of skeleton weed (*Chondrilla juncea L.*) shown by electrical parameters. J Exp Bot 31:967–974
Greenham CG, Randall PL, Muller WJ (1982) Studies of phosphorus and potassium deficiencies in Trifolium subterraneum based on electrical measurements. Can J Bot 60:634–644
Havriliak S, Negami S (1966) A complex plane analysis of α-dispersions in some polymer systems. J Polym Sci: Part C 14:99–117
Hayden RI, Moyse CA, Calder FW, Crawford DP, Fensom DS (1969) Electrical impedance studies on potato and alfalfa tissue. J Exp Bot 20:177–200
Kanai H, Haeno M, Sakamoto K (1987) Electrical measurement of fluid distribution in legs and arms. Med Prog Technol 12: 159–170
Macdonald JR (1987) Impedance spectroscopy – Emphasizing solid Materials and Systems. John Wiley & Sons, New York
Macdonald JR (1991) Impedance Spectroscopy. In: Meyers RA (ed) Encyclopedia of Physical Science and Technology, 1991 Yearbook. Academic Press, New York, pp 279–291
Markx GH, Davey CL, Kell DB (1991) To what extent is the magnitude of the Cole-Cole α of the β-dielectric dispersion of cell suspensions explicable in terms of the cell size distribution. Bioelectrochem Bioenerg 25:195–211
Mørkrid L, Qiao Z-G (1988) Continuous estimation of parameters in skin electrical admittance from simultaneous measurements at two different frequencies. Med Biol Eng Comput 26:633–640
Raistrick ID (1987) The electrical analogs of physical and chemical processes. In: Macdonald JR (ed) Impedance spectroscopy – Emphasizing Solid Materials and Systems. John Wiley & Sons, New York, pp 27–84
Repo T (1994) Influence of different electrodes and tissues on the impedance spectra of Scots pine shoots. Electro- and Magnetobiology 13:1–14
Repo T, Zhang MIN (1993) Modelling woody plant tissues using a distributed electrical circuit. J Exp Bot 44:977–982
Repo T, Zhang MIN, Ryyppö A, Vapaavuori E, Sutinen S (1994) Effects of freeze-thaw injury on parameters of distributed electrical circuits of stems and needles of Scots pine seedlings at different stages of acclimation. J Exp Bot 45:823–833
Schanne OF, P.-Ceretti ER (1978) Impedance measurements in biological cells. John Wiley & Sons, New York
Soikkeli S (1981) Comparsion of cytological injuries in conifer needles from several polluted industrial environments in Finland. Ann Bot Fenn 18:47–61
Thomas BJ, Cornish BH, Ward LC (1992) Bioelectrical impedance analysis for measurement of body fluid volumes: a review. J Clin Eng 17:505–510
Zhang MIN, Willison JHM (1991) Electrical impedance analysis in plant tissues: A double shell model. J Exp Bot 42:1465–1475
Zhang MIN, Willison JHM (1993) Electrical impedance anlysis in plant tissues: Impedance measurement in leaves. J Exp Bot 44:1369–1375

Appendix 1. Membrane transmission line property in Scots pine needles

For an infinitely long transmission line, as shown in Fig. 3, the two circuits in Figs. 8 and 9 are equivalent. If we use Z_t to represent the impedance of the circuit in Fig. 8, there is the following relationship between the two circuits:

$$\frac{1}{Z_t} = \frac{1}{R_4 + Z_t} + \frac{1}{R_3} + j\omega C \tag{A-1}$$

$$Z_t = \frac{1}{2}\left[\left(R_4^2 + \frac{4R_4 R_3}{1 + j\omega CR_3}\right)^{0.5} - R_4\right] \tag{A-2}$$

Since R_3 is typically very large (i.e. $R_3 >> R_4$) we get by R_4 approaching zero,

$$Z_t \simeq \left(\frac{R_4 R_3}{1 + j\omega CR_3}\right)^{0.5} \tag{A-3a}$$

or

$$Z_t \simeq \frac{A_o}{(1 + j\omega\tau_m)^{0.5}} \tag{A-3b}$$

in which $A_o = (R_4 R_3)^{0.5}$ and $\tau_m = CR_3$.

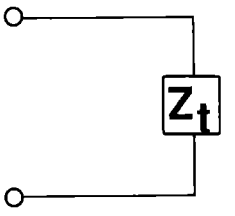

Fig. 8. A distributed circuit with Z_t equal to the total transmission line property

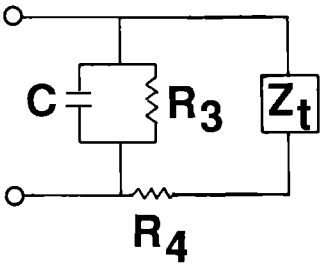

Fig. 9. The same distributed circuit as in Fig. 8, but written in a form which includes C, R_3 and R_4

Appendix 2. Frequency response properties of (A-3b)

The normalized form of (A-3b) is

$$Z = \frac{1}{(1 + j\omega\tau_m)^{0.5}} \tag{A-3c}$$

(i) At extremely high frequency: both resistance (Z') and reactance (Z'') approach zero.
(ii) At extremely low frequency: Z' is 1 and Z'' is zero.
(iii) To find the characteristic frequency (f_c) at which $-Z''$ is maximal, let

$$U = \left[1 + (\omega\tau_m)^2\right]^{0.5} \tag{A-4}$$

then

$$-Z'' = \frac{(U-1)^{0.5}}{2^{0.5}U} \tag{A-5}$$

From $d(-Z'')/dU = 0$, we get

$$U = 2 \tag{A-6}$$

and then

$$\omega\tau_m = 3^{0.5} \tag{A-7a}$$

or

$$f_c' = 3^{0.5}(2\pi\tau_m)^{-1} \tag{A-7b}$$

At this characteristic frequency, $Z' = (3/8)^{0.5}$ and $-Z'' = (1/8)^{0.5}$.

Appendix 3. The relationship between the circuit element in Fig. 4 A and the circuit element in Fig. 4 B (see Cole 1928, p. 34; Macdonald 1987, p. 11)

Conversion of Fig. 4 A circuit to 4 B circuit:

$$R_\infty = \frac{R_1 R_2}{R_1 + R_2} \tag{A-8a}$$

$$R_o = R_\infty + \frac{R_1^2}{R_1 + R_2} \tag{A-8b}$$

$$Z_2 = \frac{Z_1}{(1 + R_2 / R_1)^2} \tag{A-8c}$$

or

$$Z_2 = \frac{2A_0'(m/n)}{(1 + j\omega\tau_m)^{0.5}} \tag{A-8d}$$

in which

$$A_0' = \frac{A_o}{(1 + R_2 / R_1)^2} \tag{A-8e}$$

(see (4) for reference).